Title Page

Title

Astronaut Kinematics and Injury Risk for Piloted Lunar Landings and Launches while Standing

Authors

Mitesh Lalwala[1,2], Bharath Koya[1,2], Karan S. Devane[1,2], Fang-Chi Hsu[3], Keegan M. Yates[4], Nathaniel J. Newby[4], Jeffrey T. Somers[5], F. Scott Gayzik[1,2], Joel D. Stitzel[1,2], and Ashley A. Weaver[1,2].

[1]Wake Forest School of Medicine, Department of Biomedical Engineering
575 N. Patterson Ave, Suite 530, Winston-Salem, NC 27101, USA.

[2]Virginia Tech-Wake Forest Center for Injury Biomechanics.
575 N. Patterson Ave, Suite 530, Winston-Salem, NC 27101, USA.

[3]Wake Forest School of Medicine, Department of Biostatistics and Data Science
525 Vine Street, Winston-Salem, NC 27101, USA.

[4]KBR.
2400 NASA Parkway, Houston, TX 77058, USA.

[5]NASA Johnson Space Center.
2101 NASA Parkway, Houston, TX 77058, USA.

Abbreviated Title

Astronauts in the standing posture for lunar missions

Correspondence

Ashley A. Weaver, Ph.D.

575 N. Patterson Ave, Suite 530, Winston-Salem, NC 27101.
Tel #: 336-716-0944.
Fax #: 336-702-9177.
Email - asweaver@wakehealth.edu

Abstract

During future lunar missions, astronauts may be required to pilot vehicles while standing, and the associated kinematic and injury response is not well understood. In this study we used human body modeling to predict unsuited astronaut kinematics and injury risk for piloted lunar launches and landings in the standing posture. Three pulses (2-5 *g*; 10–150 ms rise times) were applied in 10 directions (vertical; ±10-degree offsets) for a total of 30 simulations. Across all simulations, motion envelopes were computed to quantify displacement of the astronaut's head (max 9.0 cm forward, 7.0 cm backward, 2.1 cm upward, 7.3 cm downward, 2.4 cm lateral) and arms (max 25 cm forward, 35 cm backward, 15 cm upward, 20 cm downward, 20 cm lateral). All head, neck, lumbar, and lower extremity injury metrics were within NASA's tolerance limits, except tibia compression forces (0–1543 N upper tibia; 0–1482 N lower tibia; tolerance—1350 N) and revised tibia index (0.04–0.58 upper tibia; 0.03–0.48 lower tibia; tolerance—0.43) for the 2.7 *g*/150 ms pulse. Pulse magnitude and duration contributed over 80% to the injury metric values, whereas loading direction contributed less than 3%. Overall, these simulations suggest piloting a lunar lander vehicle in the standing posture presents a low risk of injury to the astronaut, although risk of tibia injury is potentially outside NASA's acceptance limits and warrants further investigation.

Keywords –

Finite element modeling, Human body model, Moon, Spaceflight, GHBMC, Biomechanics, Injury criteria, Motion envelope, Effect size

Abbreviations

2.7 *g*/150 ms	Half-sinusoidal pulse with 2.7 *g* (26.5 m/s^2) peak acceleration and 150 ms rise time
2 *g*/50 ms	Half-sinusoidal pulse with 2 *g* (19.6 m/s^2) peak acceleration and 50 ms rise time
5 *g*/10 ms	Half-sinusoidal pulse with 5 *g* (49 m/s^2) peak acceleration and 10 ms rise time
ACL	Anterior Cruciate Ligament
AIS	Abbreviated Injury Scale
Ant-Post	Anterior-Posterior
ATD	Anthropomorphic Test Device
BrIC	Brain Injury Criterion
CG	Center of Gravity
FE	Finite Element
GHBMC	Global Human Body Model Consortium
HBM	Human Body Model
HIC	Head Injury Criterion
IARV	Injury Assessment Reference Value
LCL	Lateral Collateral Ligament
M50-PS	GHBMC average-male simplified pedestrian model
MCL	Medial Collateral Ligament
NASA	National Aeronautics and Space Administration
N_{ij}	Neck Injury Criterion
PCL	Posterior Cruciate Ligament
PMHS	Post-Mortem Human Subject
RTI	Revised Tibia Index

Introduction

The National Aeronautics and Space Administration (NASA) is planning to send the first woman and next man to the Moon by 2024.[14] NASA is currently investigating key transformative technologies that will enable humans to conduct long-duration exploration of the Moon and future missions to Mars. One of the major concerns for future space missions is the safety of crewmembers. Spaceflight launch and landings are critical phases of a space mission, involving large amounts of energies and transient accelerations. Although most of these energies are absorbed and dissipated by the space vehicle, some amount of kinetic energy is transmitted to the occupant aboard the vehicle, which can impose high dynamic loads.[2] The risk of injury to astronauts from these dynamic loads are not completely understood.[22] Dynamic loads can jeopardize the entire space mission if they impair an astronaut's ability to perform their mission duties, or compromise the astronaut's ability to egress the vehicle during an emergency. NASA's Human Research Program must characterize the injury response of astronauts under spaceflight-related dynamic loading conditions, and establish injury assessment reference values (IARVs) for spaceflight applications that will mitigate the total risk of injury to an acceptable level.[15,16]

Because the Moon's gravity is about one-sixth of Earth's gravity, a possibility exists that astronauts may pilot a lunar transfer vehicle in a standing posture (similar to the Apollo missions), rather than a conventional seated posture necessary during Earth Landings.[29] In the standing posture, the astronauts will have a better view of the landing and launch sites, making it easier for them to control the launch and landing phases on the lunar surface. In addition, the standing posture can also help reduce the space and material requirements of the landing vehicle, which are 2 of the most constrained resources for space missions. However, the response of the human body in a standing posture under dynamic loading conditions is not well understood and requires further investigation. In addition, the current design reference missions may require astronauts to stay at least 10 days in microgravity before they land on the Moon, which can lead to some physiological deconditioning resulting in a decreased tolerance to dynamic loads.[2,37]

Astronauts of lunar missions will be subjected to complex multi-directional dynamic loads in the standing posture that are drastically different from the loads encountered in terrestrial vehicles. Hence, IARVs developed for automotive and military applications on Earth cannot be directly translated for space missions.[15,16,36] Injury risk curves for space applications that are derived by conventional tests on volunteers, post-mortem human subjects (PMHS), or anthropomorphic test devices (ATD) are expensive and difficult to conduct.[2,22,36] Due to difficulties associated with getting PMHS and ATD inside the spacesuit, tests using PMHS and ATD also have limitations for assessing spacesuit safety. Therefore, new innovative tools and techniques are needed to assess occupant response in the wide variety of loading conditions encountered during space missions.[17] Recent studies have shown that the computational finite element (FE) human body models (HBM) can provide an effective means for studying astronaut response under multi-directional loading conditions in a time- and cost-efficient manner.[7,10,33]

Computational HBMs are anatomical models of the human body developed from multimodality medical images and anthropomorphic data from volunteers, and they are used to study the response of the human body under dynamic loading conditions.[8] The constitutive material behavior for these models is derived from localized biomechanical testing on PMHS or on animals. These models are emerging as a cost- and time-efficient alternative to PMHS and ATDs for studying injury mechanisms in a wide variety of applications. These types of models include the Global Human Body Models Consortium (GHBMC) FE HBMs, which are gaining credibility for identifying and understanding injury mechanisms under dynamic loading conditions in automotive,[4,24] sports,[1,5] aerospace,[10,33] and military[9,27] environments. The GHBMC models have been previously validated for multidirectional loading conditions similar to those induced by space missions,[7] and can be used for assessing astronaut response during lunar launch and landing in the standing posture.

The objectives of the current study were to develop a computational modeling method for simulating the response of standing astronauts subjected to lunar launch and landing using the GHBMC HBM, and to assess the effects of different acceleration pulses and loading directions on kinematics and injury risk.

Materials and Methods

Positioning

The standing posture of the astronaut was simulated using the GHBMC average-male simplified pedestrian model M50-PS (v1.5.2). The original M50-PS model in a walking stance was repositioned into a neutral standing posture using a series of dynamic simulations. After repositioning, the model was gravity-settled on the ground (lunar gravity: 1.63 m/s^2) to ensure the feet were well-rested on the ground. Because the Apollo crews used foot harnesses, the model was restrained to the ground using foot harnesses (Figure 1).

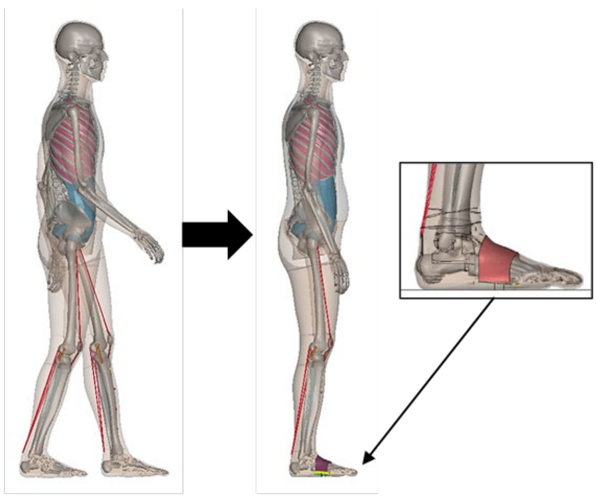

Figure 1. The initial walking stance of the GHBMC M50-PS model (left) was repositioned into the neutral standing posture (right) to represent the standing posture of the astronaut. The inset picture represents the well-rested position of feet on the ground in the final posture and in the foot harness.

Dynamic Simulations

Lunar gravity was simulated by applying 1.63 m/s^2 acceleration in a vertically downward direction throughout the simulation. Dynamic loading conditions related to lunar launch and landing were simulated by applying a half-sinusoidal acceleration pulse[2,29] with varied peak acceleration and rise time to the ground. Based on lunar transient acceleration literature,[29] 3 different pulses were selected to represent loading conditions related to nominal and off-nominal scenarios: (1) 2 g (19.6 m/s^2) peak acceleration pulse with 50 ms rise time, “2 g/50 ms”; (2) 2.7 g (26.5 m/s^2) peak acceleration pulse with 150 ms rise time, “2.7 g/150 ms”; and (3) 5 g (49 m/s^2) peak acceleration pulse with 10 ms rise time, “5 g/10 ms” (Appendix A, Figure A1). The load was applied in 5 different directions—vertical and ± 10° offset in the anterior-posterior and lateral directions (Figure 2) to simulate possible off-axis variation in the loading direction from the vertical axis due to vehicle orientation and lunar topography.

For all the loading directions and pulses, simulations were carried out in 2 conditions: (1) when the ground was moving towards the model, called “towards” polarity hereafter, and (2) when the ground was moving away from the model, called “away” polarity hereafter. The ground (of the vehicle) would be moving towards the occupant (inertial response of the astronaut towards the ground) during both launch and landing because in both conditions the vehicle is accelerating away from the surface of the moon. However, if the vehicle landing pads or restraint systems are underdamped, astronauts may experience rebounding force resulting in the ground (of the vehicle) moving away from the occupant (inertial response of astronaut away from the ground). A total of 30 simulations were conducted using LS-Dyna R9.3.1 (ANSYS, Inc., Livermore, CA): 3 pulses (2 g/50 ms, 2.7 g/150 ms, 5 g/10 ms; Figure A1) × 2 polarities (away; towards) × 5 directions (Figure 2). Simulations with shorter duration pulses (5 g/10 ms; 2 g/50 ms; Figure A1) were conducted for additional 50 ms after the dynamic acceleration pulse under lunar gravity without any external loads to ensure peak values for different metrics were fully achieved.

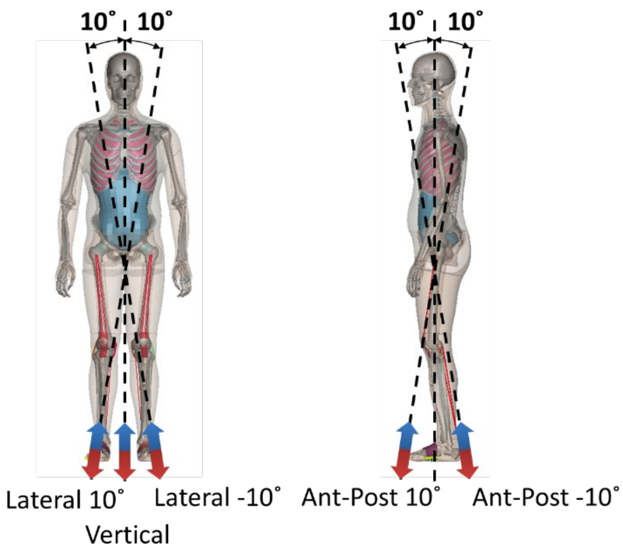

Figure 2. Dynamic simulation setup for lunar launch and landing in the standing posture with the 5 different loading directions. Blue arrows represent a "towards" polarity where the ground is moving towards the model and red arrows represent an "away" polarity where the ground is moving away from the model.

Data Processing

Head and arm kinematics and the injury metrics in Table 1 were extracted from the simulations using standard instrumentation defined for the GHBMC models. A total of 19 injury metrics were extracted (note the tibia compression force and revised tibia index were evaluated at 2 locations: the upper tibia and the lower tibia). The peak value of each metric was extracted within the dynamic loading time phase: 300 ms for the 2.7 *g*/150 ms pulse, 150 ms for the 2 *g*/50 ms pulse, and 70 ms for the 5 *g*/10 ms pulse. These peak metrics were compared against IARVs from the literature and NASA's acceptable risk levels (Table 1).

Table 1. Body region injury metrics and corresponding injury risk

Region	Injury Metric	Injury Risk Function	IARV
Head	Linear Acceleration	Concussion[26]	10g
	Rotational Acceleration*	Concussion[21]	2200 rad/s^2
	Head Injury Criterion (HIC_{15})*	Head Injury[18]	340
	Brain Injury Criterion (BrIC)	Brain Injury[31]	0.12
Neck	Axial Compression Force*	Cervical Spine Fracture[35]	1100 N
	Axial Tension Force*	Distraction Injury[35]	1097 N
	Flexion Moment*	Wedge Fracture[13,20]	96 Nm
	Extension Moment*		39 Nm
	Neck Injury Criterion, N_{ij}	Neck Injury[19]	0.16
Lumbar	Axial Compression Force*	Vertebra Fracture[34]	5300 N
Lower Extremities	Femur Axial Compression Force	Femur Fracture[12]	2400 N
	Ligament Forces†	Ligament rupture/avulsion[3,11,23]	Anterior Cruciate Ligament (ACL): 1725 N Posterior Cruciate Ligament (PCL): 1627 N Medial Collateral Ligament (MCL): 1215 N Lateral Collateral Ligament (LCL): 571 N
	Upper/Lower Tibia Compression Force	Tibia Plateau Fracture[12]	1350 N
	Upper/Lower Tibia – Revised Tibia Index (RTI)	Tibia Shaft Fracture[12]	0.43

Injury assessment reference values (IARV) represent 1% risk of Abbreviated Injury Scale (AIS) 2+ injury unless otherwise mentioned. *IARV for the injury metric taken from Somers et al. (2017)[28]. †IARV represents ligament rupture/avulsion injury.

Loading Parameter Effect Size

Statistical analysis was conducted to assess the relative association of acceleration pulse (magnitude and rise time) and loading direction on different injury metrics. To develop a linear regression model, all the injury metrics were individually regressed against 3 loading condition variables simultaneously: pulse-type (categorical variable – 2 *g*/50 ms, 2.7 *g*/150 ms, 5 *g*/10 ms), and anterior-posterior and lateral loading angles (continuous variables) using JMP Pro v13.0 (SAS, Cary, NC). Because this is a pilot study, only the main effects were included in the model. Separate models were developed for away versus towards polarity loading conditions for each injury metric. From these regression models, R^2 and partial-R^2 values were extracted for each injury metric. The R^2 value indicates the percentage of the total variation in the injury metric explained by pulse-type and loading directions. Similarly, the partial-R^2 represents a contribution of the given loading variable on the observed variation of the injury metric after adjusting for the other loading variables, where a higher partial-R^2 indicates a greater effect. Because 19 different injury metrics were regressed from the same 30 simulations, a significance level $\alpha = 0.0026$ (=0.05/19) after Bonferroni correction was used.

Results

Body Kinematics and Injury Metrics

Head

For the away polarity, all head injury metric peaks were observed for the 2.7 *g*/150 ms pulse ($p < 0.0001$) (Figure 3; Figure A2). For the towards polarity, the head center of gravity (CG) linear acceleration and HIC_{15} were highest for the 2 *g*/50 ms pulse ($p < 0.0001$), whereas the brain injury criterion (BrIC) value was highest for 2.7 *g*/150 ms pulse ($p < 0.0001$). For most of the simulations, the loading directions had minimal effect on the head injury metrics, as indicated by narrow error bars. Head injury metrics for all the loading conditions were well below the IARV tolerance limits (Appendix B, Table B1-Table B4).

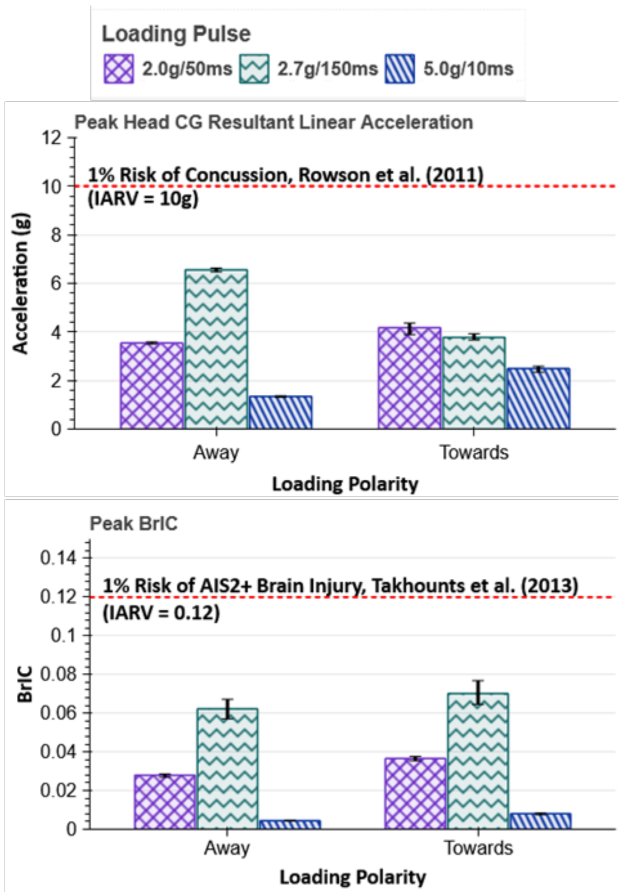

Figure 3. Comparison of the peak head center of gravity (CG) resultant linear acceleration and brain injury criterion (BrIC) injury metrics. Each bar represents the average of the peak values for the given pulse in all the loading directions. Error bars represent the maximum and minimum values observed in the group. IARV: injury assessment reference value. AIS: Abbreviated Injury Scale.

Displacement of the head CG relative to the base of the neck (T1 vertebrae) was compared for different loading conditions (Figure 4; Figure A3; Figure A4). Maximum head displacements were observed for the 2.7 *g*/150 ms pulse due to comparatively more loading time and energy transferred (Figure 4). For the away polarity, the head moved backward and upward during all the loading scenarios. The head moved as much as 7.0 cm backward and 2.1 cm upward for loading in the away polarity. However, not much lateral head displacement was observed for these loading conditions. For the toward polarity, the head moved forward and downward during all the loading conditions. The head moved as much as 9.0 cm forward, 7.3 cm downward, and 2.4 cm in the lateral direction for the towards polarity loading. Initially, similar head trajectories were observed for all the loading directions and only minor effects of anterior-posterior and lateral loading angle were observed on the final position of the head. For the 5 *g*/10 ms and 2 *g*/50 ms pulses, head kinematics followed similar trends but with reduced magnitude of displacement due to comparatively less loading time.

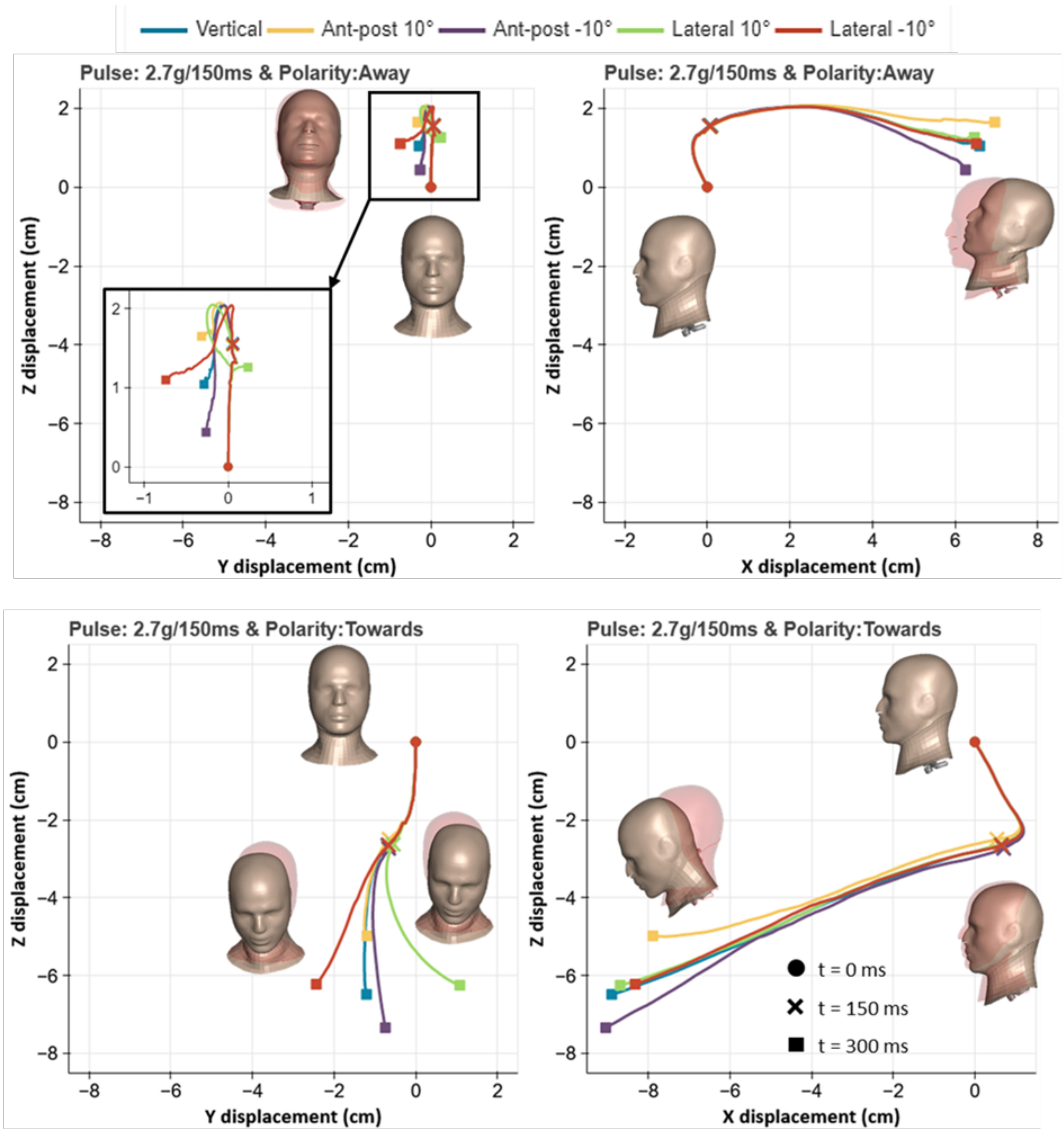

Figure 4. Head displacement for the 2.7 *g*/150 ms pulse in different loading directions. The solid model represents the head position at a given time and the transparent model represents the head position at t=0 ms.

Neck and Lumbar Spine

Similar to the injury metrics for the head, all the neck and lumbar spine injury metrics were lower than the IARVs for all the loading conditions (Figure 5; Figure A5; Table B5 –Table B10). Both the neck and lumbar spine were loaded in tension for the away polarity, and were loaded in compression for the towards polarity. In general, all the neck and lumbar injury metrics were higher for the 2.7 *g*/150 ms pulse than the other loading pulses. The anterior-posterior or lateral offset in the loading direction showed no significant effect on the neck and lumbar injury metrics for all the loading conditions as evidenced by narrow error bars.

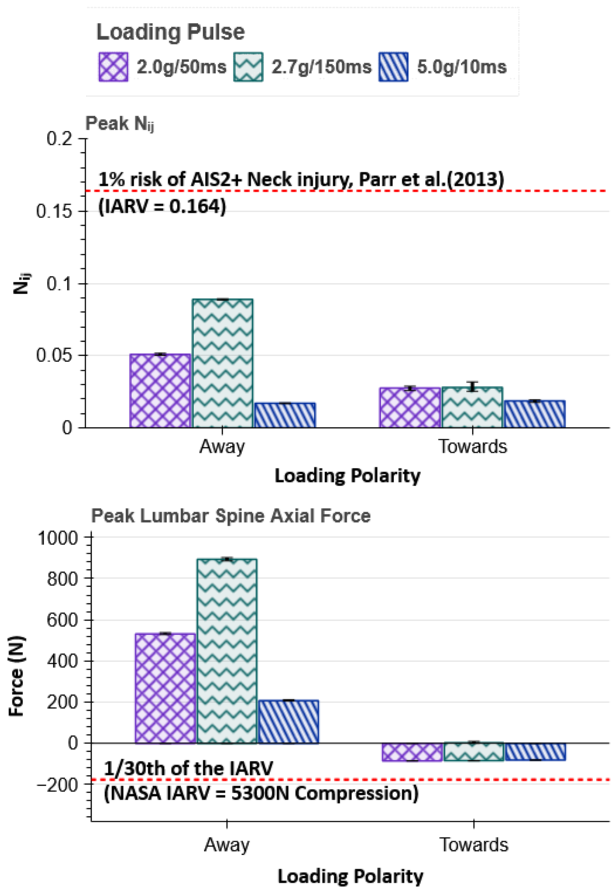

Figure 5. Comparison of the neck injury criterion (N_{ij}) and lumbar spine axial force injury metrics. Each bar represents the average of the peak values for the given pulse in all the loading directions. Error bars represent the maximum and minimum values observed in the group. IARV: injury assessment reference value. AIS: Abbreviated Injury Scale.

Lower Extremities

The lower extremities were subjected to tensile loading in the away polarity and to compressive loading in the towards polarity (Figure 6). For all the loading conditions, the 2.7 *g*/150 ms pulse produced higher injury metrics for the lower extremity than did the other 2 pulses (Table B11–Table B15). Axial compression forces of the upper (1543 N) and lower (1482 N) tibia exceeded the 1350 N IARV for 10° off-axis loading in the anterior-posterior direction for the 2.7 *g*/150 ms pulse in the towards polarity. Similarly, the revised tibia index (RTI) that includes both tibia axial compressive loads and bending moments exceeded the 0.43 IARV for both the upper and lower tibia for the 2.7 *g*/150 ms pulse in the towards polarity across vertical and off-axis loading directions (RTI: 0.43–0.58 upper; 0.36–0.48 lower). Overall, higher values of RTI were observed for the towards polarity than the away polarity (upper tibia, $p = 0.0005$ and lower tibia, $p = 0.0001$).

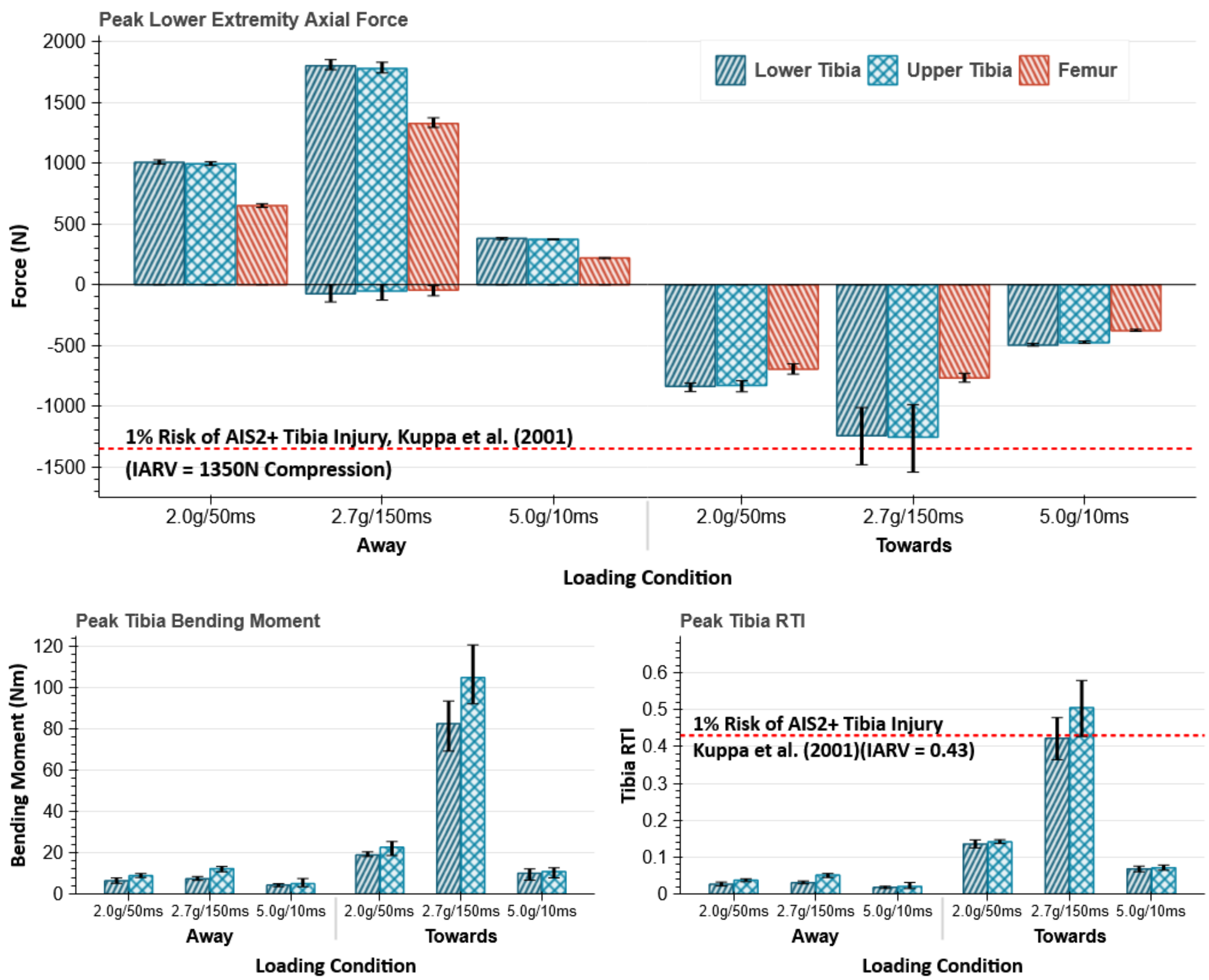

Figure 6. Comparison of the femur and tibia injury metrics. Each bar represents the average of the peak values for the given pulse in all the loading directions. Error bars represent the maximum and minimum values observed in the group. IARV: injury assessment reference value. AIS: Abbreviated Injury Scale.

Knee ligaments underwent tensile forces during all the loading conditions (Figure 7), except for the Anterior Cruciate Ligament (ACL) in the towards polarity due to knee-buckling (Figure A8). For all the loading conditions, maximum forces were observed in the ACL, followed by the forces in the Posterior Cruciate Ligament (PCL), Medial Collateral Ligament (MCL), and Lateral Collateral Ligament (LCL), successively. All the forces were below the ligament rupture forces reported in literature[3,11,23] (Table B16 – Table B20).

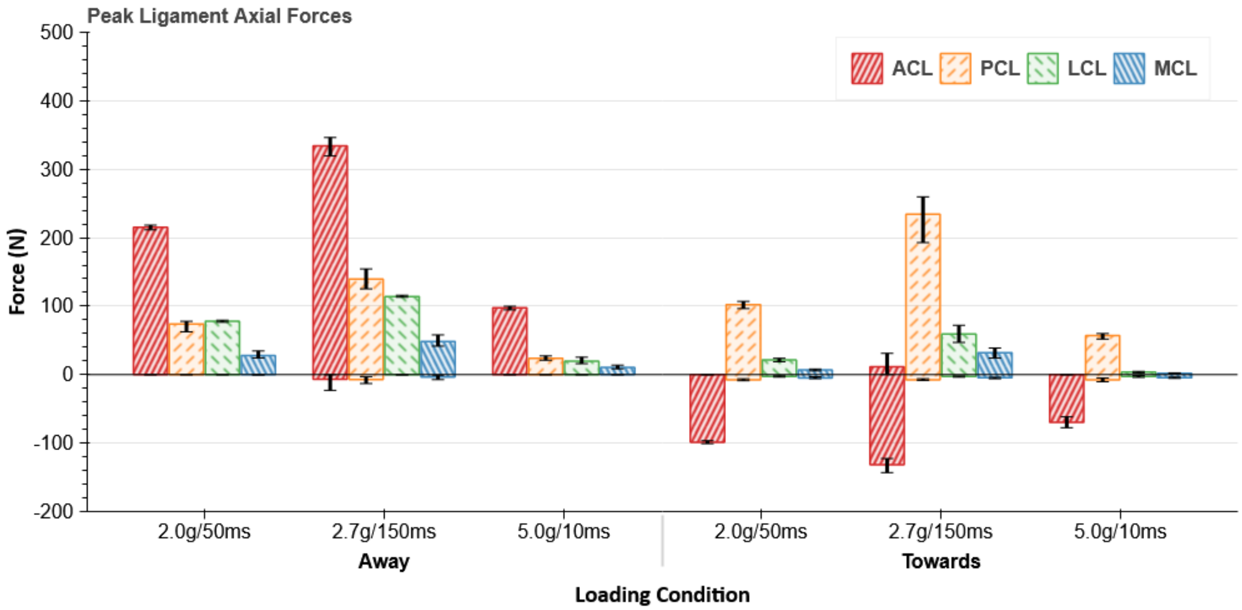

Figure 7. Comparison of the knee ligament forces for the anterior cruciate ligament (ACL), posterior cruciate ligament (PCL), lateral collateral ligament (LCL), and medial collateral ligament (MCL). Each bar represents the average of the peak values for the given pulse in all the loading directions. Error bars represent the maximum and minimum values observed in the group.

Upper Extremities

Arm motion envelopes for all the loading conditions were plotted (Figure 8; Figure A6; Figure A7). Similar to the head kinematics, maximum arm motion was observed from the 2.7 *g*/150 ms pulse due to comparatively more loading time (Figure 8). For the away polarity, the arms moved upward and forward, whereas for the towards polarity the arms moved downward and backward. The arms moved as much as 25 cm forward, 15 cm upward, and 20 cm laterally for the away polarity loading. For the towards polarity loading, the arms moved as much as 35 cm backward, 20 cm downward, and 10 cm laterally. Significant effects of loading directions were observed for both the away and the towards loading conditions.

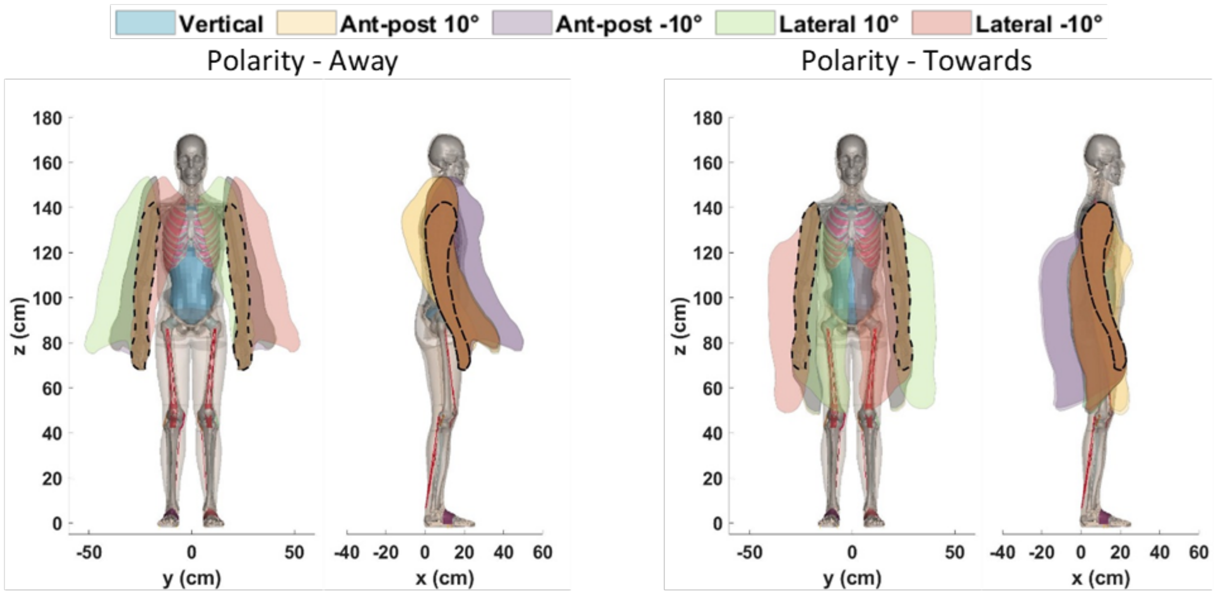

Figure 8. Arm motion envelops for the 2.7 *g*/150 ms pulse for different loading directions.

Statistical Analysis Results

For the away polarity, the loading condition parameters explained more than 90% of the observed variation in statistical significance for all the injury metrics, except for neck compression force and flexion moment and lower extremities compression forces (Table 2). For the away polarity, the associations between all these injury metrics and loading parameters were statistically significant. The injury metrics showed maximum dependency (average 80%) on the nature of the pulse magnitude and duration, and least dependency on the loading direction (~1% for the anterior-posterior direction and 0.5% for the lateral direction). Similarly, for the towards polarity, the loading condition parameters explained an average 90% of the variation observed for all the injury metrics (Table 3). For the towards polarity, the associations between loading parameters and the injury metrics were all statistically significant, except for head rotational acceleration, neck tension force, and ACL tension. Again, the maximum variation (~88%) was contributed to the nature of the pulse, and the loading directions had little effect (~2%) on the injury metrics.

Table 2. The effect size (R^2 and partial-R^2) for different loading parameters in the away polarity on injury metrics.

Injury Metric	**Partial-R^2**			**R^2**
	Pulse	**Ant-Post Loading Angle**	**Lateral Loading Angle**	
Head Linear Acceleration	**100.0%**	0.0%	0.0%	**100.0%**
Head Rotational Acceleration	**99.5%**	0.0%	0.0%	**99.5%**
Head Injury Criterion (HIC_{15})	**99.9%**	0.0%	0.0%	**99.9%**
Brain Injury Criterion (BrIC)	**99.4%**	0.3%	0.0%	**99.6%**
Neck Axial Compression Force	14.3%	17.9%	0.0%	32.1%
Neck Axial Tension Force	**100.0%**	0.0%	0.0%	**100.0%**
Neck Extension Moment	**100.0%**	0.0%	0.0%	**100.0%**
Neck Flexion Moment	8.3%	0.0%	1.2%	9.5%
Nij	**100.0%**	0.0%	0.0%	**100.0%**
Lumbar Spine Compression Force	**99.8%**	0.0%	0.0%	**99.8%**
Femur Compression Force	47.4%	0.1%	0.0%	47.5%
Upper Tibia Compression Force	42.8%	0.9%	1.0%	44.6%
Lower Tibia Compression Force	59.5%	0.7%	1.5%	61.7%
Upper Tibia Revised Tibia Index (RTI)	**89.3%**	0.9%	2.2%	**92.4%**
Lower Tibia Revised Tibia Index (RTI)	**77.7%**	0.1%	0.6%	**78.4%**
Anterior Cruciate Ligament Tension	**99.7%**	0.0%	0.1%	**99.8%**
Posterior Cruciate Ligament Tension	**97.6%**	0.2%	1.1%	**98.9%**
Lateral Collateral Ligament Tension	**99.7%**	0.0%	0.0%	**99.8%**
Medial Collateral Ligament Tension	**94.1%**	0.3%	1.5%	**95.8%**
Average	80.5%	1.1%	0.5%	82.1%

Bold and Underlined values are statistically significant with Bonferroni correction.

Table 3. The effect size (R^2 and partial-R^2) for different loading parameters in the towards polarity on injury metrics.

Injury Metric	Partial-R^2			R^2
	Pulse	Ant-Post Loading Angle	Lateral Loading Angle	
Head Linear Acceleration	**97.1%**	1.6%	0.1%	**98.8%**
Head Rotational Acceleration	36.8%	10.8%	0.0%	47.6%
Head Injury Criterion (HIC_{15})	**98.4%**	**1.0%**	0.1%	**99.5%**
Brain Injury Criterion (BrIC)	**99.2%**	0.3%	0.0%	**99.5%**
Neck Axial Compression Force	**96.2%**	1.5%	0.1%	**97.8%**
Neck Axial Tension Force	51.0%	3.3%	4.7%	59.0%
Neck Extension Moment	**99.9%**	0.1%	0.0%	**100.0%**
Neck Flexion Moment	**99.9%**	0.0%	0.0%	**99.9%**
Nij	**88.0%**	0.1%	0.1%	**88.2%**
Lumbar Spine Compression Force	**98.9%**	0.5%	0.2%	**99.6%**
Femur Compression Force	**98.1%**	1.0%	0.0%	**99.1%**
Upper Tibia Compression Force	**90.0%**	2.2%	0.1%	**92.3%**
Lower Tibia Compression Force	**91.7%**	1.7%	0.2%	**93.6%**
Upper Tibia Revised Tibia Index (RTI)	**97.6%**	0.9%	0.0%	**98.5%**
Lower Tibia Revised Tibia Index (RTI)	**97.2%**	0.7%	0.0%	**97.9%**
Anterior Cruciate Ligament Tension	42.3%	0.4%	2.6%	45.3%
Posterior Cruciate Ligament Tension	**95.7%**	0.1%	0.9%	**96.6%**
Lateral Collateral Ligament Tension	**95.4%**	0.1%	1.5%	**97.0%**
Medial Collateral Ligament Tension	**93.1%**	0.6%	0.5%	**94.2%**
Average	87.7%	1.4%	0.6%	89.7%

Bold and Underlined values are statistically significant with Bonferroni correction.

Discussion

The injury metric and kinematic data generated from these computational simulations characterize the expected response of an astronaut piloting a vehicle during lunar launches or landings in a standing posture. The injury metrics indicated the probability of injury under given loading conditions, and we compared these metrics with established IARVs to identify the relative risk of injuries. During an exploration mission, astronauts will have limited access to medical care, so even a minor injury can have huge negative consequences such as loss of mission or loss of life. Hence, to minimize safety risk for astronauts, NASA has set a 1% risk tolerance of AIS2+ injury for nominal launch and landing scenarios,[28] which is significantly lower than the risk tolerance used for automotive IARVs (Table A1).

For the current study, most of the IARVs for head, neck, and lumbar injury metrics (marked by * in Table 1) were taken from a NASA technical report,[28] and are based on previously reported data in the literature. For the remaining injury metrics, IARVs were defined as the injury metric value corresponding to 1% AIS2+ injury risk, calculated using the injury risk curve provided in the corresponding literature. The IARV for linear acceleration of the head CG was determined from instrumented helmet research on football players.[26] The BrIC IARV was determined from the injury curve reported in Takhounts et al. (2013).[31] Similarly, for the neck injury metric, N_{ij}, IARV was calculated using the risk curve provided by Parr et al. (2013),[19] which is based on sled test data using human volunteers. IARVs for the lower extremities were determined by using risk functions published by Kuppa et al. (2001).[12] Because injury risk curves are not available for knee ligaments, the peak force values were directly compared against ligament failure values reported in the literature.[3,11,23]

Overall, all injury metric values except for tibia axial compression force and RTI were less than the IARVs for all the loading conditions, indicating acceptable injury risk for all the body regions, except the tibia, for lunar launches and landings piloted in a standing posture.

For the head injury metrics, head CG linear accelerations of 3.8 ± 2.2 *g* for the away polarity and 3.5 ± 0.8 *g* (mean±SD) for the towards polarity are less than the 10 *g* IARV. In absence of direct transfer of energy to the head, very low HIC_{15} values of 0.5 ± 0.6 and 0.3 ± 0.1 were determined for the away and the towards polarities, values well under the IARV of 340. Similarly, head CG rotational accelerations of 42 ± 28 rad/s^2 and 73 ± 30 rad/s^2 for the away and the towards polarities, respectively, are significantly less than the IARV of 2200 rad/s^2, and corresponding BrIC values of 0.03 ± 0.02 and 0.04 ± 0.03 are also less than the IARV of 0.12. More linear acceleration-related loading was observed for the away polarity, whereas more rotational acceleration-related loading was observed for the towards polarity. In the away polarity, the model is pulled in the direction of the loading, leading to tensile loading in the neck with some neck extension, and resulting in higher linear acceleration-related injury metrics. In the towards polarity, the model is pushed in the direction of the loading, resulting in neck flexion with head rotation, and leading to higher rotational injury metric values. These head injury metric values are comparable to risk of injury when jumping from a 30 cm height (3.9 ± 1.2 *g*, 68 ± 37 rad/s^2, and HIC_{15} 0.4 ± 0.3),[6] which indicates a very low risk of head injury risk under lunar loading conditions.

As mentioned earlier, for loading in the away polarity, the neck was loaded in tension (209 ± 127 N) and extension (3.0 ± 1.6 Nm) due to stretching of the neck and backward rotation of the head, resulting in an N_{ij} of 0.05 ± 0.03. In the towards polarity, the neck was loaded in compression (128 ± 23 N) and flexion (2.9 ± 2.3 Nm) due to forward rotation of the head, resulting in a N_{ij} of 0.02 ± 0.00. All values for neck injury are lower than the IARVs. Similar to the head injury metrics, the neck injury metrics are comparable to risk of injury when jumping from a 30 cm height (175 ± 60 N compression, 6.0 ± 2.5 Nm extension, and 0.05 ± 0.01 N_{ij})[6], indicating the risk of neck injury during lunar loading conditions are similar to the risk of incurring a neck injury during everyday activities. However, the away polarity has a lower margin of safety to the IARVs than the towards polarity, indicating comparatively higher risk of neck injury in the away polarity.

As with the neck, the lumbar spine experienced tensile forces (544.16 ± 290.23 N) in the away polarity and compression forces (84.01 ± 1.77 N) in the towards polarity. These lumbar compressive forces are much lower than the IARV of 5300 N. Rohlmann et al. (2014)[25] reported that lifting a weight from the ground can induce 304–1649 N load in the lumbar spine, whereas upper body flexion can produce 341–1075 N load in the lumbar spine. Hence, the lumbar loads observed in the current study are within the range of everyday activities.

Of all the body regions, the lower extremities had the highest risk of injury, with some metrics exceeding the IARVs (Figure 6). In all the loading conditions, the upper and lower tibia underwent similar axial forces: 1048 ± 595 N tension in the upper tibia and 1062 ± 602 N tension in the lower tibia in the away polarity, and 854 ± 347 N compression in the upper tibia and 860 ± 329 N compression in the lower tibia in the towards polarity. However, axial forces observed in the femur, 731 ± 472 N tension in the away polarity and 615 ± 177 N compression in the towards polarity, were comparatively lower than tibia forces for all the cases, indicating some amount of energy being absorbed or dissipated in the knee joint.

All the femur compression forces were less than the IARV of 2400 N. However, upper and lower tibia compression forces of 1543 and 1482 N, respectively, exceeded the IARV of 1350 N in the 10° offset anterior-posterior direction with the 2.7 *g*/150 ms pulse in the towards polarity, indicating unacceptable fracture risk. As for lower extremity bone distraction forces, no injury metric comparisons were found. However, Taylor et al. (2020)[32] reported that daily activities induce axial distraction forces of 205 ± 53 N in the femur and 82 ± 35 N in the tibia. The axial tension forces we observed in the away polarity are significantly higher than these values (731 ± 472 N), indicating the need for further investigation.

To assess fracture risk, we calculated the RTI, which is a function of tibia axial compression force and total bending moment, for the upper and lower tibia, and compared values to the IARV. RTI values were lower for the away polarity (0.04 ± 0.01 upper tibia and 0.00 ± 0.01 lower tibia) and higher for the towards polarity (0.24 ± 0.20 upper tibia and 0.21±0.16 lower tibia). Both the upper and lower tibia RTI exceeded the IARV limit of 0.43 for the 2.7 *g*/150 ms pulse in the towards polarity in vertical and off-axis loading directions, indicating that lunar launch and landings piloted in a standing posture may have more risk of tibia injury than the tolerance threshold set by NASA. RTI values followed the same trend as tibia bending moments, and high RTI values were due to the high amount of bending generated in the tibia due to knee-buckling in the towards polarity (Figure A8). This risk of tibia injury in a standing posture could be mitigated by an effective restraint system that can offload the lower extremities and prevent excessive knee buckling.

In the away polarity, all the knee ligaments underwent tensile loads due to relative movement between the femur and tibia. In the towards polarity, the ACL underwent compression force whereas all the remaining ligaments underwent tension. Overall, for the away polarity, the ACL underwent the maximum force (216 ± 100 N), followed by the PCL and LCL undergoing similar forces (71 ± 40 N and 79 ± 50 N, respectively), and the MCL undergoing the least force (29 ± 17 N). For the towards polarity, initially the ACL received maximum force during the loading phase of the pulse (100 ± 27 N compression), but due to knee-buckling maximum loads were transferred to the PCL during the unloading phase (131 ± 80 N tension). Relatively low tensile forces were observed in the LCL and MCL (28 ± 25 and 14 ± 14 N) for the towards polarity. Knee ligaments underwent higher forces in the away compared to the towards polarity. These forces were all less than the ligament failure loads reported in the literature (1725 N for ACL,[3] 1627 N for PCL,[23] 571 N for LCL,[12] and 1215 N for MCL[12]). However, these reported values correspond to complete ligament rupture or avulsion, and astronauts could still experience ligament stretching or minor tears at comparatively lower loads. However, in absence of relevant data, further investigation is required to quantify the risk of injury to astronauts' knee ligaments.

Our regression analyses revealed that most of the injury metrics are more associated with the nature of the loading (the magnitude and the duration of the pulse), and relatively less associated with the anterior-posterior and lateral offset in the loading directions from the vertical. This indicates that, to control the injury risk, it is more important to control the loading rate than the loading direction.

In additional to comparing injury metrics, we assessed the kinematic response of astronauts in terms of the relative displacement of the head CG and arm motion envelopes. These kinematic responses of the head and arms are important to consider when designing future spacesuits, helmets, and space vehicles. We determined that the head can move from 7.0 cm backward to 9.0 cm forward, 2.1 cm upward to 7.3 cm downward, and 2.4 cm laterally across all the loading directions. If the head moves excessively it could impact the spacesuit helmet, which can cause concussion or other head injuries. Hence, these displacements should be considered when designing spacesuit helmets. Similarly, arm motion can cause flail injuries from interaction between the astronaut's body and surrounding interior of the space vehicle. The kinematic arm motion envelopes determined in the current study can aid with designing the interiors of space vehicles to avoid flail injuries during launch or landing.

The models used in the current study did not include active musculature, which is a limitation. Active musculature could alter the kinematic response and knee buckling observed under the dynamic loading for the longer duration pulses. Apollo astronauts have reported that landing and lift-off from the lunar surface raises a large amount of lunar dust, affecting the visibility of the launch and landing sites.[30] Due to impaired visibility, it is difficult for the astronaut to identify the exact moment of landing, and therefore they may have a delayed response to these dynamic events. Under these conditions, the response predicted by the passive model may still be applicable and can serve as a baseline for future lunar simulation studies incorporating muscle activation.

Another limitation of our model is the lack of a full restraint system. Because the restraint system design for upcoming lunar missions is still under development, we simulated only minimal restraints. Similarly, since the design and properties of astronaut suits and helmets are not publicly available, our simulations did not include suits or helmets. Although this approach is far from reality, it gives a more conservative estimate of astronaut response in the absence of any protective equipment, and the results serve as a baseline for future in-depth studies incorporating protective gear and restraint systems.

IARVs were determined by extrapolating the published injury risk curve to 1% injury risk values. However, injury risk curves are developed from injurious experimental tests, and may not be as accurate for lower probabilities of injury risk. Hence, a need exists to determine injury metric values that correspond to lower injury risk related to spaceflight. However, based on the risk curve data currently available, the results of this study give an approximation of injury risk expected across a variety of lunar launch and landing events.

Although astronauts landed on the Moon in a standing posture during the Apollo missions, not much data from these missions is available to understand the effects on astronaut kinematics and injury risks. This simulation study has overcome this difficulty by generating predictive body kinematic and injury risk for astronauts in a standing posture under lunar mission launch- and landing-related dynamic loading conditions. The data generated will also serve as baseline data for identifying potential injury mechanisms for upcoming lunar missions and help in developing effective protective gear, restraint systems, and vehicle interiors to minimize injury risk in astronauts. FE simulation is the best current strategy available for assessing injury risk in this scenario, and the method developed here can be used to make comparisons between different suit and restraint design approaches.

Acknowledgments

This study was supported by a NASA Human Research Program Student Augmentation Award to NASA Grant No. NNX16AP89G. Views expressed are those of the authors and do not represent the views of the GHBMC, NASA, or KBR. All simulations were run on the Distributed Environment for Academic Computing (DEAC) high-performance computing cluster at Wake Forest University with the support of Cody Stevens and Adam Carlson.

Disclosure

Dr. Stitzel and Dr. Gayzik are members of Elemance, LLC, which provides academic and commercial licenses of the GHBMC-owned human body computer models.

References

1. Bruneau, D. A., and D. S. Cronin. Brain response of a computational head model for prescribed skull kinematics and simulated football helmet impact boundary conditions. *J. Mech. Behav. Biomed. Mater.* 115:104299, 2021.

2. Caldwell, E., M. Gernhardt, J. T. Somers, D. Younker, and N. Newby. Evidence Report: Risk of Injury Due to Dynamic Loads. National Aeronautics and Space Administration, Houston, Texas, 2012, 1–55 pp.

3. Caplan, N., and D. F. Kader. Biomechanical analysis of human ligament grafts used in knee-ligament repairs and reconstructions. In *Classic Papers in Orthopaedics*. London: Springer London, pp. 145–147, 2014.

4. Costa, C., J. Aira, B. Koya, W. Decker, J. Sink, S. Withers, R. Beal, S. Schieffer, S. Gayzik, J. Stitzel, and A. Weaver. Finite element reconstruction of a vehicle-to-pedestrian impact. *Traffic Inj. Prev.* 0:1–3, 2020.

5. Decker, W. B., D. A. Jones, K. Devane, M. L. Davis, J. P. Patalak, and F. S. Gayzik. Simulation-based assessment of injury risk for an average male motorsport driver. *Traffic Inj. Prev.* 1–6, 2020.

6. Funk, J. R., J. M. Cormier, C. E. Bain, H. Guzman, E. Bonugli, and S. J. Manoogian. Head and neck loading in everyday and vigorous activities. *Ann. Biomed. Eng.* 39:766–776, 2011.

7. Gaewsky, J. P., D. A. Jones, X. Ye, B. Koya, K. P. McNamara, F. S. Gayzik, A. A. Weaver, J. B.

Putnam, J. T. Somers, and J. D. Stitzel. Modeling human volunteers in multidirectional, uni-axial sled tests using a finite element human body model. *Ann. Biomed. Eng.* 47:487–511, 2019.

8. Gayzik, F. S., D. P. Moreno, C. P. Geer, S. D. Wuertzer, R. S. Martin, and J. D. Stitzel. Development of a full body CAD dataset for computational modeling: A multi-modality approach. *Ann. Biomed. Eng.* 39:2568–2583, 2011.

9. Hostetler, Z. S., J. Aira, J. D. Stitzel, and F. S. Gayzik. A computational study of the biomechanical response of the human lower extremity subjected to high rate vertical accelerative loading. *IRCOBI Annu. Meet. Proc.* 662–673, 2019.

10. Jones, D. A., J. P. Gaewsky, J. T. Somers, F. S. Gayzik, A. A. Weaver, and J. D. Stitzel. Head injury metric response in finite element ATDs and a human body model in multidirectional loading regimes. *Traffic Inj. Prev.* 20:S96–S102, 2019.

11. Kerrigan, J. R., B. J. Ivarsson, D. Bose, N. J. Madeley, S. A. Millington, K. S. Bhalla, and J. Crandall. Rate-sensitive constitutive and failure properties of human collateral knee ligaments. *Proc. 2003 IRCOBI Conf.* 177–190, 2003.at <http://www.ircobi.org/wordpress/downloads/irc0111/2003/Session3/3.4.pdf>

12. Kuppa, S., J. Wang, M. Haffner, and R. Eppinger. Lower extremity injuries and associated injury criteria. *SAE Tech. Pap.* 4:, 1-15, 2001.

13. Mertz, H. J. Injury risk assessments based on dummy responses. In *Accidental Injury*, edited by A. M. Nahum, and J. W. Melvin. New York, NY: Springer, New York, pp. 89–102,

2002.

14. National Aeronautics and Space Administration. NASA’s lunar exploration program overview, 2020. <https://www.nasa.gov/sites/default/files/atoms/files/artemis_plan-20200921.pdf>

15. National Aeronautics and Space Administration. HRR - Gap - OP-101, 2021.at <https://humanresearchroadmap.nasa.gov/Gaps/gap.aspx?i=740#>

16. National Aeronautics and Space Administration. HRR - Gap - OP-201, 2021.at <https://humanresearchroadmap.nasa.gov/Gaps/gap.aspx?i=741>

17. National Aeronautics and Space Administration. HRR - Gap - OP-301, 2021.at <https://humanresearchroadmap.nasa.gov/gaps/gap.aspx?i=742>

18. National Highway Traffic Safety Administration. Final economic assessment, FMVSS No. 201, upper interior head protection. *Off. Regul. Anal. Plans Policy. Washingt. DC* , 1995.

19. Parr, J. C., M. E. Miller, J. A. Pellettiere, and R. A. Erich. Neck injury criteria formulation and injury risk curves for the ejection environment: A pilot study. *Aviat. Space. Environ. Med.* 84:1240–1248, 2013.

20. Patrick, L. M., and C. C. Chou. Response of the human neck in flexion, extension and lateral flexion, 1976.at <https://trid.trb.org/view/61565>

21. Pellman, E. J., D. C. Viano, A. M. Tucker, I. R. Casson, and J. F. Waeckerle. Concussion in professional football: reconstruction of game impacts and injuries. *Neurosurgery* 53:799–812; discussion 812-4, 2003.

22. Pintar, F., P. Ivancic, M. Kleinberger, and J. Rupp. Research plan review for: The risk of injury from dynamic loads final report. , 2015.at <https://humanresearchroadmap.nasa.gov/reviews/>

23. Prietto, M. P., J. R. Bain, S. N. Stonebrook, and R. A. Settlage. Tensile strength of the human posterior cruciate ligament (PCL). *Trans Orthop Res Soc* 13:736–745, 1988.

24. Ramachandra, R., V. Pradhan, Y. Kang, R. Davidson, M. Humer, and J. Zhang. Evaluate the Effect of Seat Back Restriction on Head, Neck and Torso Responses of Front Seat Occupants when Subjected to a Moderate Speed Rear-Impact. *SAE Tech. Pap. Ser.*, 2021.

25. Rohlmann, A., D. Pohl, A. Bender, F. Graichen, J. Dymke, H. Schmidt, and G. Bergmann. Activities of everyday life with high spinal loads. *PLoS One* 9:e98510, 2014.

26. Rowson, S., and S. M. Duma. Brain injury prediction: Assessing the combined probability of concussion using linear and rotational head acceleration. *Ann. Biomed. Eng.* 41:873–882, 2013.

27. Somasundaram, K., L. Zhang, D. Sherman, P. Begeman, D. Lyu, and J. M. Cavanaugh. Evaluating thoracolumbar spine response during simulated underbody blast impact using a total human body finite element model. *J. Mech. Behav. Biomed. Mater.* 100:103398, 2019.

28. Somers, J. T., D. Gohmert, and J. W. Brinkley. Application of the Brinkley dynamic response criterion to spacecraft transient dynamic events. *NASA Tech. Memo.* , 2017.at <http://ston.jsc.nasa.gov/collections/trs/_techrep/TM-2013-217380.pdf>

29. Somers, J. T., T. Reiber, J. Pattarini, N. Newby, and P. Greenhalgh. Lunar transient accelerations white paper. *NASA Tech. Memo.* 1–17, 2020.at <https://ntrs.nasa.gov/citations/20205008198>

30. Stubbs, T. J., R. R. Vondrak, and W. M. Farrell. Impact of dust on lunar exploration. *ESA - Work. Dust Planet. Syst.* 239–243, 2007.at <https://www.nasa.gov/centers/johnson/pdf/486014main_StubbsImpactOnExploration.4075.pdf>

31. Takhounts, E. G., M. J. Craig, K. Moorhouse, J. McFadden, and V. Hasija. Development of brain injury criteria (BrIC). *SAE Tech. Pap.* 2013-Novem:243–266, 2013.

32. Taylor, C. E., Y. Zhang, Y. Qiu, H. B. Henninger, K. B. Foreman, and K. N. Bachus. Estimated forces and moments experienced by osseointegrated endoprostheses for lower extremity amputees. *Gait Posture* 80:49–55, 2020.

33. Ye, X., D. A. Jones, J. P. Gaewsky, B. Koya, K. P. McNamara, M. Saffarzadeh, J. B. Putnam, J. T. Somers, F. S. Gayzik, J. D. Stitzel, and A. A. Weaver. Lumbar spine response of computational finite element models in multidirectional spaceflight landing conditions. *J. Biomech. Eng.* 142:, 2020.

34. Yoganandan, N., M. W. J. Arun, B. D. Stemper, F. A. Pintar, and D. J. Maiman. Biomechanics of human thoracolumbar spinal column trauma from vertical impact loading. *Ann. Adv. Automot. Med. Assoc. Adv. Automot. Med. Annu. Sci. Conf.* 57:155–66, 2013.

35. Yoganandan, N., S. Chirvi, F. A. Pintar, A. Banerjee, and L. Voo. Injury Risk Curves for the Human Cervical Spine from Inferior-to-Superior Loading. *SAE Tech. Pap.* 2019-Novem:271–292, 2018.

36. Institute of Medicine 2014. Review of NASA's Evidence reports on human health risks: 2013 letter report. Washington, DC: The National Academies Press, 2014, 1–52 pp.doi:10.17226/18575

37. National Academies of Sciences, Engineering, and Medicine 2016. Review of NASA's evidence reports on human health risks: 2015 Letter Report. Washington, D.C.: Washington, DC: The National Academies Press, 2016, 1–82 pp.doi:10.17226/21844

Appendix A

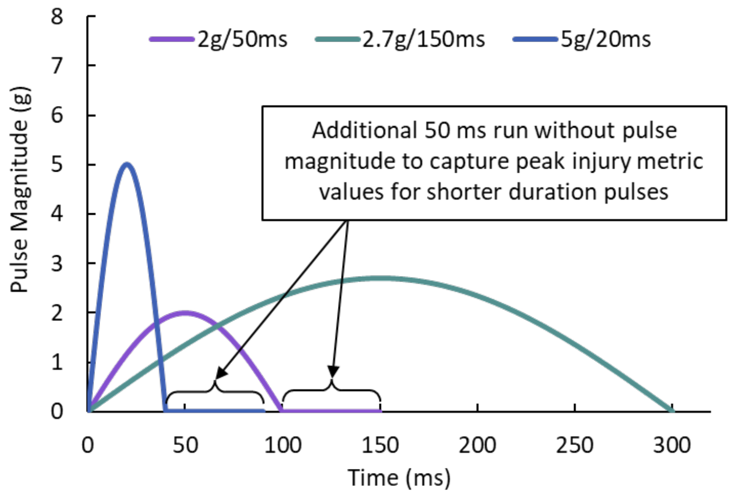

Figure A1. Dynamic loading pulses used for simulating lunar launch and landing conditions.

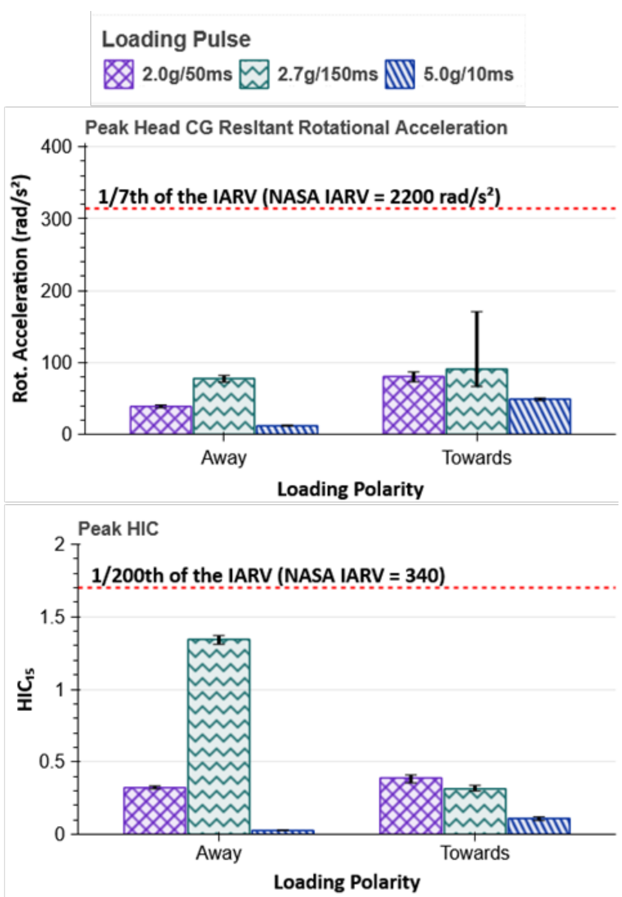

Figure A2. Comparison of the peak head center of gravity (CG) resultant rotational acceleration and head injury criterion (HIC_{15}) injury metrics. Each bar represents the average of the peak values for the given pulse in all the loading directions. Error bars represent the maximum and minimum values observed in the group. IARV: injury assessment reference value.

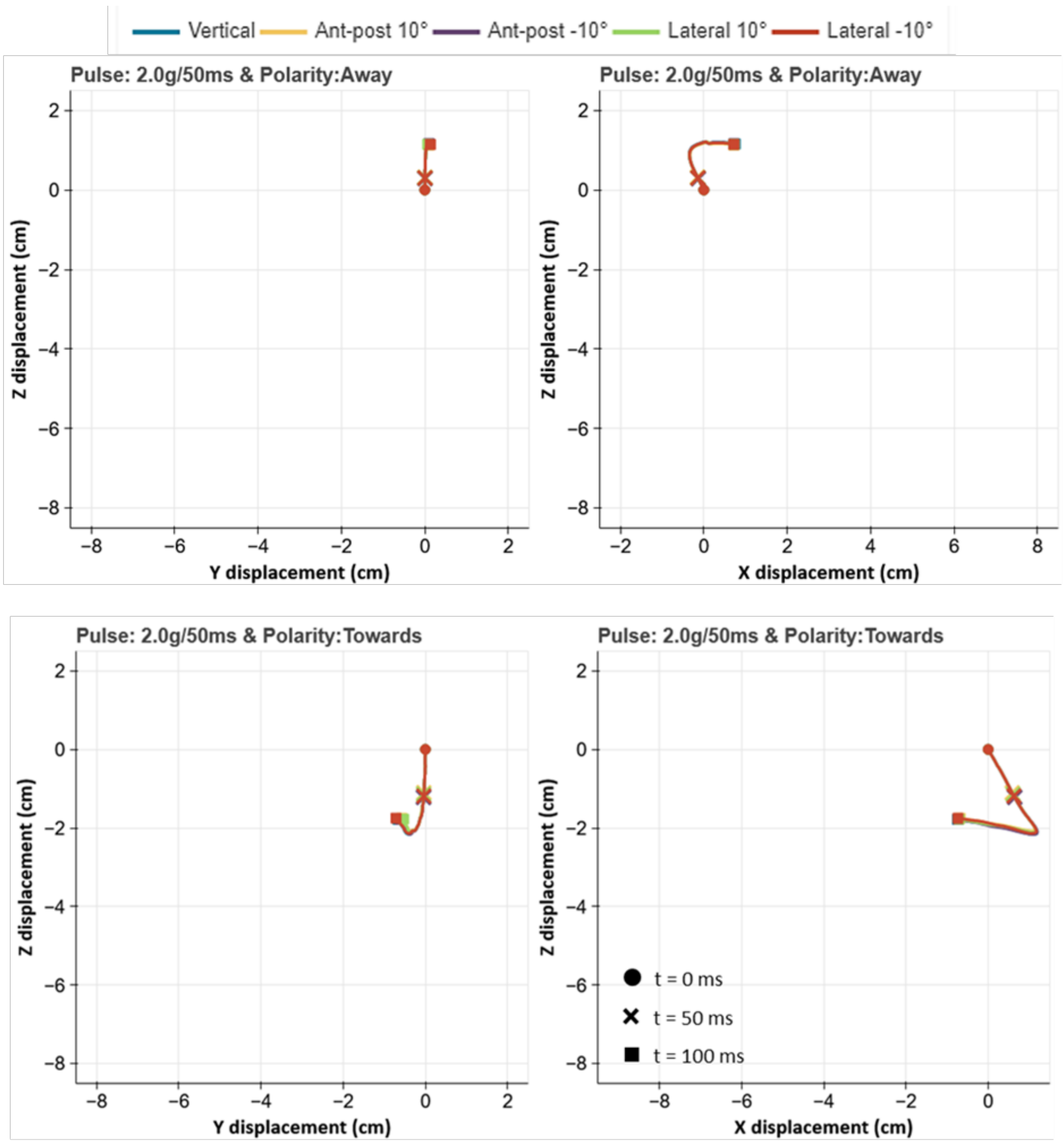

Figure A3. Head displacement for the 2 *g*/50 ms pulse in different loading directions.

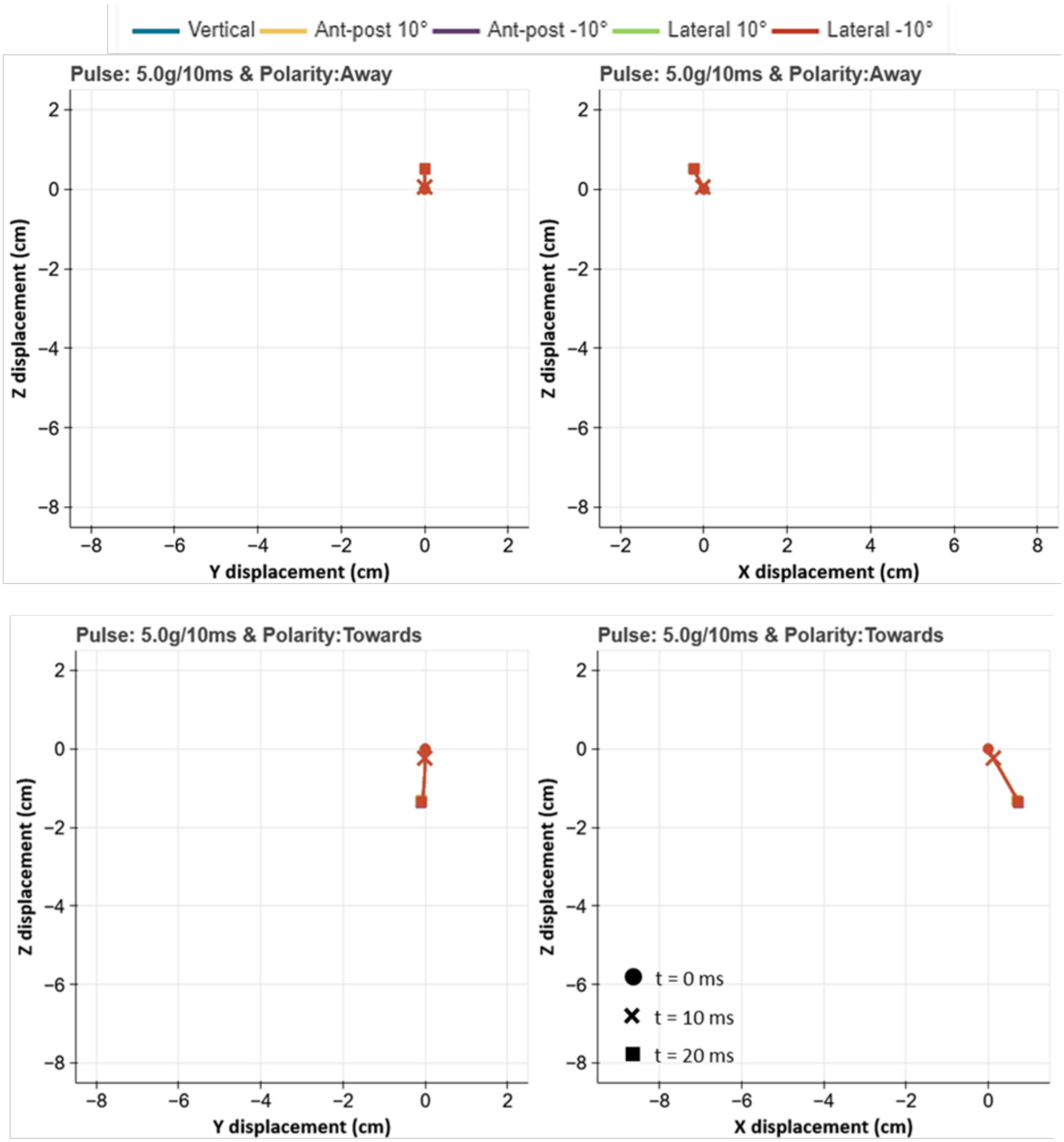

Figure A4. Head displacement for the 5 g/10 ms pulse in different loading directions.

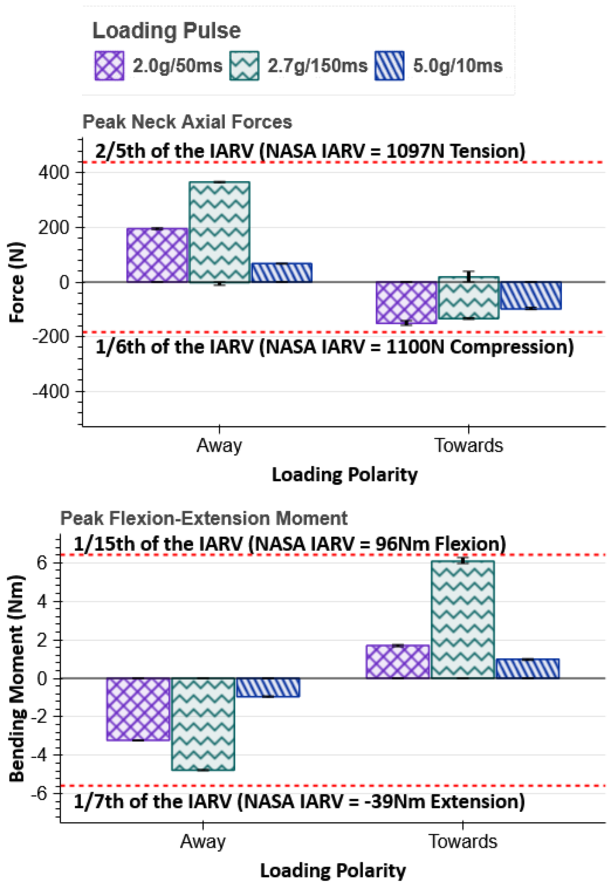

Figure A5. Comparison of the peak neck axial forces and flexion-extension moments injury metrics. Each bar represents the average of the peak values for the given pulse in all the loading directions. Error bars represent the maximum and minimum values observed in the group. IARV: injury assessment reference value

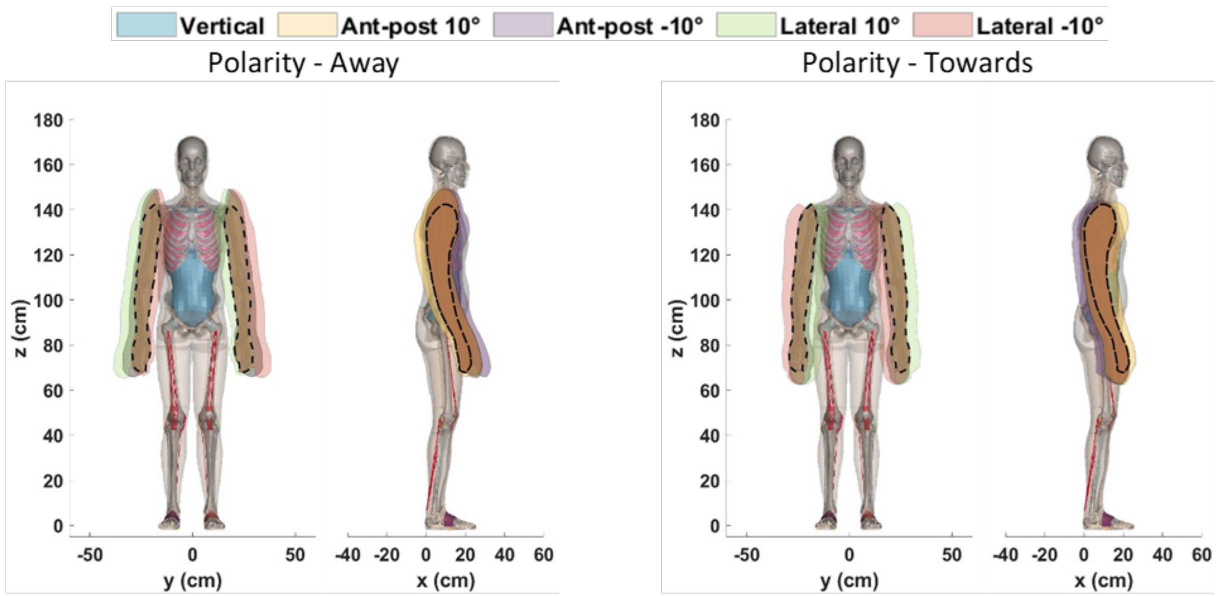

Figure A6. Arm motion envelops for the 2 g/50 ms pulse for different loading directions.

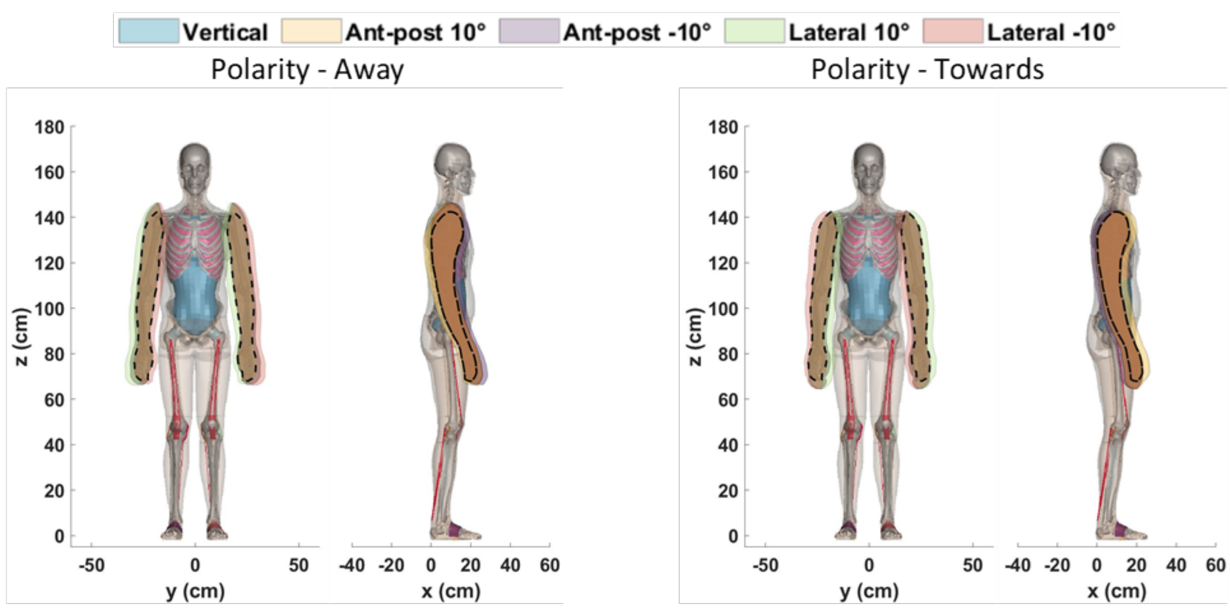

Figure A7. Arm motion envelops for the 5 g/10 ms pulse for different loading directions.

Table A1. Comparison of IARVs for automotive versus aerospace applications.

Region	Injury Metric	IARV for Automotive Applications Insurance Institute of Highway Safety [1]	IARV Used in This Aerospace Study[2-6]
Head	Resultant Linear Acceleration (g)	70	10
	Rotational Acceleration (rad/s^2)	-	2200
	Head Injury Criterion (HIC_{15})	700	340
	Brain Injury Criterion (BrIC)	-	0.12
Neck	Axial Compression Force (N)	3200	1100
	Axial Tension Force (N)	4000	1097
	Flexion Moment (Nm)	-	96
	Extension Moment (Nm)	-	39
	Neck Injury Criterion, N_{ij}	1.00	0.16
Lumbar	Axial Compression Force (N)	-	5300
Lower Extremities	Femur Compression Force (N)	9100	2400
	Tibia Compression Force (N)	8000	1350
	Revised Tibia Index (RTI)	1.00	0.43

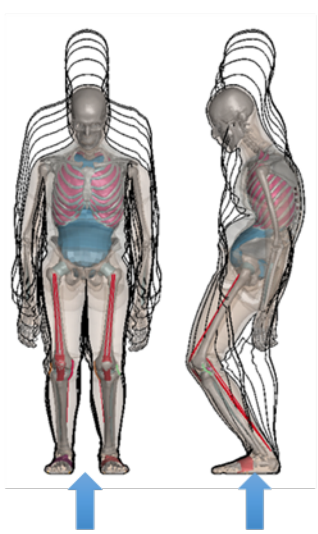

Figure A8. Knee buckling and spinal slouching for towards polarity loading in the vertical direction for the 2.7 *g*/150 ms pulse.

Bibliography

1. Insurance Institute for Highway Safety. Moderate Overlap Frontal Crashworthiness Evaluation Guidelines for Rating Injury Measures. , 2014.at <https://www.iihs.org/media/dcc9d5d6-c301-4f92-a7b5-dad13ffc7766/6h8G8A/Ratings/Protocols/current/measures_frontal.pdf>

2. Kuppa, S., J. Wang, M. Haffner, and R. Eppinger. Lower extremity injuries and associated injury criteria. *SAE Tech. Pap.* 4:, 2001.

3. Parr, J. C., M. E. Miller, J. A. Pellettiere, and R. A. Erich. Neck Injury Criteria Formulation and Injury Risk Curves for the Ejection Environment: A Pilot Study. *Aviat. Space. Environ. Med.* 84:1240–1248, 2013.

4. Rowson, S., and S. M. Duma. Brain Injury Prediction: Assessing the Combined Probability of Concussion Using Linear and Rotational Head Acceleration. *Ann. Biomed. Eng.* 41:873–882, 2013.

5. Somers, J. T., D. Gohmert, and J. W. Brinkley. Application of the Brinkley Dynamic Response Criterion to Spacecraft Transient Dynamic Events. *NASA Tech. Memo.* , 2017.at <http://ston.jsc.nasa.gov/collections/trs/_techrep/TM-2013-217380.pdf>

6. Takhounts, E. G., M. J. Craig, K. Moorhouse, J. McFadden, and V. Hasija. Development of Brain Injury Criteria (BrIC). SAE Tech. Pap. 2013-Novem:243–266, 2013.

Appendix B

Injury metric results from the 30 simulations. Injury assessment reference value (IARV) represents 1% risk of Abbreviated Injury Scale (AIS)2+ injury unless otherwise mentioned. Values exceeding the IARV are bolded and designated by cell shading.

Table B1. Injury Metric – Head Center of Gravity (CG) Linear Acceleration (g) (IARV = 10g)

Loading Polarity		Away			Towards		
Loading Pulse		2.0g/50ms	2.7g/150ms	5.0g/10ms	2.0g/50ms	2.7g/150ms	5.0g/10ms
Loading Direction	Vertical	3.59	6.63	1.37	4.31	3.79	2.54
	Ant-Post 10°	3.53	6.47	1.31	3.89	3.78	2.34
	Ant-Post -10°	3.57	6.57	1.37	4.37	3.92	2.58
	Lateral 10°	3.50	6.56	1.34	4.05	3.67	2.46
	Lateral -10°	3.51	6.53	1.32	4.22	3.69	2.50
Mean		3.54	6.55	1.34	4.17	3.77	2.49
Std		0.03	0.05	0.02	0.18	0.09	0.08

Table B2. Injury Metric – Head CG Rotational Acceleration (rad/s2) (IARV = 2200 rad/s^2)

Loading Polarity		Away			Towards		
Loading Pulse		2.0g/50ms	2.7g/150ms	5.0g/10ms	2.0g/50ms	2.7g/150ms	5.0g/10ms
Loading Direction	Vertical	38.47	78.79	12.22	86.91	73.32	50.10
	Ant-Post 10°	40.85	72.54	12.76	72.86	170.55	46.82
	Ant-Post -10°	36.84	81.99	11.24	82.48	66.43	50.25
	Lateral 10°	38.53	78.00	11.95	76.77	72.77	49.52
	Lateral -10°	38.82	77.08	11.84	82.59	70.78	48.20
Mean		38.70	77.68	12.00	80.32	90.77	48.98
Std		1.28	3.06	0.49	4.93	39.96	1.30

Table B3. Injury Metric – Head Injury Criterion (HIC_{15}) (IARV = 340)

Loading Polarity		Away			Towards		
Loading Pulse		2.0g/50ms	2.7g/150ms	5.0g/10ms	2.0g/50ms	2.7g/150ms	5.0g/10ms
Loading Direction	Vertical	0.33	1.37	0.03	0.41	0.32	0.12
	Ant-Post 10°	0.31	1.37	0.03	0.35	0.30	0.09
	Ant-Post -10°	0.33	1.33	0.03	0.40	0.34	0.12
	Lateral 10°	0.32	1.31	0.03	0.38	0.30	0.11
	Lateral -10°	0.32	1.34	0.03	0.40	0.31	0.11
Mean		0.32	1.34	0.03	0.39	0.31	0.11
Std		0.01	0.02	0.00	0.02	0.01	0.01

Table B4. Injury Metric – Brain Injury Criterion (BrIC) (IARV = 0.12)

Loading Polarity		Away			Towards		
Loading Pulse		2.0g/50ms	2.7g/150ms	5.0g/10ms	2.0g/50ms	2.7g/150ms	5.0g/10ms
Loading Direction	Vertical	0.03	0.06	0.00	0.04	0.07	0.01
	Ant-Post 10°	0.03	0.06	0.00	0.04	0.06	0.01
	Ant-Post -10°	0.03	0.07	0.00	0.04	0.08	0.01
	Lateral 10°	0.03	0.06	0.00	0.04	0.07	0.01
	Lateral -10°	0.03	0.06	0.00	0.04	0.07	0.01
Mean		0.03	0.06	0.00	0.04	0.07	0.01
Std		0.00	0.00	0.00	0.00	0.00	0.00

Table B5. Injury Metric – Neck Axial Compression Force (N) (IARV = 1100 N)

Loading Polarity		Away			Towards		
Loading Pulse		2.0g/50ms	2.7g/150ms	5.0g/10ms	2.0g/50ms	2.7g/150ms	5.0g/10ms
Loading Direction	Vertical	-0.07	-0.07	-0.07	-156.79	-133.45	-101.31
	Ant-Post 10°	-0.07	-0.07	-0.07	-141.52	-136.15	-93.06
	Ant-Post -10°	-0.07	-12.11	-0.07	-158.64	-136.88	-101.28
	Lateral 10°	-0.07	-0.07	-0.07	-146.43	-132.35	-99.01
	Lateral -10°	-0.07	-0.07	-0.07	-153.56	-130.64	-100.26
Mean		-0.07	-2.47	-0.07	-151.39	-133.89	-98.99
Std		0.00	4.82	0.00	6.46	2.33	3.08

Table B6. Injury Metric – Neck Axial Tension Force (N) (IARV = 1097 N)

Loading Polarity		Away			Towards		
Loading Pulse		2.0g/50ms	2.7g/150ms	5.0g/10ms	2.0g/50ms	2.7g/150ms	5.0g/10ms
Loading Direction	Vertical	198.23	368.00	68.61	0.10	39.06	0.10
	Ant-Post 10°	192.33	363.85	65.63	0.10	0.10	0.10
	Ant-Post -10°	195.78	367.49	67.81	0.10	21.18	0.10
	Lateral 10°	193.63	365.17	67.45	0.10	3.71	0.10
	Lateral -10°	195.12	363.88	66.20	0.10	28.77	0.10
Mean		195.02	365.68	67.14	0.10	18.56	0.10
Std		2.00	1.76	1.08	0.00	14.78	0.00

Table B7. Injury Metric – Neck Flexion Moment (Nm) (IARV = 96 Nm)

Loading Polarity		Away			Towards		
Loading Pulse		2.0g/50ms	2.7g/150ms	5.0g/10ms	2.0g/50ms	2.7g/150ms	5.0g/10ms
Loading Direction	Vertical	0.00	0.00	0.00	1.75	6.23	1.01
	Ant-Post 10°	0.00	0.00	0.00	1.64	6.26	0.93
	Ant-Post -10°	0.00	0.00	0.00	1.72	5.98	1.02
	Lateral 10°	0.00	0.00	0.00	1.68	5.95	0.98
	Lateral -10°	0.00	0.00	0.00	1.73	5.97	0.99
Mean		0.00	0.00	0.00	1.70	6.08	0.99
Std		0.00	0.00	0.00	0.04	0.14	0.03

Table B8. Injury Metric – Neck Extension Moment (Nm) (IARV = 39 Nm)

Loading Polarity		Away			Towards		
Loading Pulse		2.0g/50ms	2.7g/150ms	5.0g/10ms	2.0g/50ms	2.7g/150ms	5.0g/10ms
Loading Direction	Vertical	-3.25	-4.80	-0.97	0.00	0.00	0.00
	Ant-Post 10°	-3.21	-4.74	-0.98	0.00	0.00	0.00
	Ant-Post -10°	-3.22	-4.78	-0.92	0.00	0.00	0.00
	Lateral 10°	-3.21	-4.74	-0.95	0.00	0.00	0.00
	Lateral -10°	-3.21	-4.77	-0.95	0.00	0.00	0.00
Mean		-3.22	-4.77	-0.95	0.00	0.00	0.00
Std		0.02	0.02	0.02	0.00	0.00	0.00

Table B9. Injury Metric – Neck Injury Criterion (N_{ij}) (IARV = 0.16)

Loading Polarity		Away			Towards		
Loading Pulse		2.0g/50ms	2.7g/150ms	5.0g/10ms	2.0g/50ms	2.7g/150ms	5.0g/10ms
Loading Direction	Vertical	0.05	0.09	0.02	0.03	0.03	0.02
	Ant-Post 10°	0.05	0.09	0.02	0.03	0.03	0.02
	Ant-Post -10°	0.05	0.09	0.02	0.03	0.03	0.02
	Lateral 10°	0.05	0.09	0.02	0.03	0.03	0.02
	Lateral -10°	0.05	0.09	0.02	0.03	0.03	0.02
Mean		0.05	0.09	0.02	0.03	0.03	0.02
Std		0.00	0.00	0.00	0.00	0.00	0.00

Table B10. Injury Metric – Lumbar Spine Axial Compression Force (N) (IARV = 5300N)

Loading Polarity		Away			Towards		
Loading Pulse		2.0g/50ms	2.7g/150ms	5.0g/10ms	2.0g/50ms	2.7g/150ms	5.0g/10ms
Loading Direction	Vertical	-0.06	-0.10	-0.06	-85.58	-85.05	-81.90
	Ant-Post 10°	-0.06	-0.10	-0.06	-85.15	-84.86	-81.38
	Ant-Post -10°	-0.06	-0.10	-0.06	-85.58	-85.09	-81.83
	Lateral 10°	-0.06	-0.10	-0.06	-85.27	-84.87	-81.33
	Lateral -10°	-0.06	-0.10	-0.06	-85.57	-85.01	-81.69
Mean		-0.06	-0.10	-0.06	-85.43	-84.98	-81.63
Std		0.00	0.00	0.00	0.18	0.09	0.23

Table B11. Injury Metric – Femur Axial Compression Force (N) (IARV = 2400 N)

Loading Polarity		Away			Towards		
Loading Pulse		2.0g/50ms	2.7g/150ms	5.0g/10ms	2.0g/50ms	2.7g/150ms	5.0g/10ms
Loading Direction	Vertical	-0.06	-15.16	-0.02	-736.62	-781.69	-381.61
	Ant-Post 10°	-0.06	-7.19	-0.02	-650.98	-729.09	-368.03
	Ant-Post -10°	-0.07	-18.00	-0.02	-721.84	-802.90	-384.10
	Lateral 10°	-0.06	-91.02	-0.02	-667.07	-770.08	-379.37
	Lateral -10°	-0.07	-91.72	-0.02	-706.76	-761.44	-378.01
Mean		-0.06	-44.62	-0.02	-696.65	-769.04	-378.23
Std		0.00	38.34	0.00	32.54	24.34	5.50

Table B12. Injury Metric – Upper Tibia Axial Compression Force (N) (IARV = 1350 N)

Loading Polarity		Away			Towards		
Loading Pulse		2.0g/50ms	2.7g/150ms	5.0g/10ms	2.0g/50ms	2.7g/150ms	5.0g/10ms
Loading Direction	Vertical	-0.11	-7.71	-0.05	-881.93	-1219.44	-480.48
	Ant-Post 10°	-0.11	-0.76	-0.05	-790.74	-1542.75	-464.64
	Ant-Post -10°	-0.10	-34.22	-0.05	-853.56	-987.08	-483.07
	Lateral 10°	-0.11	-127.82	-0.05	-794.51	-1321.56	-483.78
	Lateral -10°	-0.11	-92.74	-0.05	-822.88	-1206.00	-477.25
Mean		-0.11	-52.65	-0.05	-828.72	-1255.37	-477.85
Std		0.01	49.62	0.00	34.91	180.38	6.99

Table B13. Injury Metric – Lower Tibia Axial Compression Force (N) (IARV = 1350 N)

Loading Polarity		Away			Towards		
Loading Pulse		2.0g/50ms	2.7g/150ms	5.0g/10ms	2.0g/50ms	2.7g/150ms	5.0g/10ms
Loading Direction	Vertical	-0.10	-107.77	-0.04	-880.26	-1215.74	-500.67
	Ant-Post 10°	-0.10	-0.77	-0.04	-808.95	-1481.51	-484.02
	Ant-Post -10°	-0.09	-36.43	-0.04	-864.73	-1012.37	-506.00
	Lateral 10°	-0.10	-142.78	-0.04	-809.84	-1321.31	-504.42
	Lateral -10°	-0.10	-89.65	-0.04	-824.70	-1180.61	-497.29
Mean		-0.10	-75.48	-0.04	-837.70	-1242.31	-498.48
Std		0.00	50.75	0.00	29.37	155.46	7.84

Table B14. Injury Metric – Upper Tibia Revised Tibia Index (RTI) (IARV = 0.43)

Loading Polarity		Away			Towards		
Loading Pulse		2.0g/50ms	2.7g/150ms	5.0g/10ms	2.0g/50ms	2.7g/150ms	5.0g/10ms
Loading Direction	Vertical	0.04	0.05	0.02	0.14	0.53	0.07
	Ant-Post 10°	0.04	0.05	0.02	0.15	0.58	0.08
	Ant-Post -10°	0.04	0.04	0.01	0.14	0.43	0.06
	Lateral 10°	0.03	0.06	0.02	0.14	0.52	0.07
	Lateral -10°	0.04	0.06	0.03	0.15	0.47	0.07
Mean		0.04	0.05	0.02	0.14	0.51	0.07
Std		0.00	0.00	0.01	0.00	0.05	0.00

Table B15. Injury Metric – Lower Tibia RTI (IARV = 0.43)

Loading Polarity		Away			Towards		
Loading Pulse		2.0g/50ms	2.7g/150ms	5.0g/10ms	2.0g/50ms	2.7g/150ms	5.0g/10ms
Loading Direction	Vertical	0.03	0.03	0.02	0.14	0.46	0.07
	Ant-Post 10°	0.02	0.03	0.02	0.13	0.48	0.08
	Ant-Post -10°	0.03	0.03	0.01	0.14	0.36	0.06
	Lateral 10°	0.03	0.04	0.02	0.12	0.43	0.07
	Lateral -10°	0.03	0.03	0.02	0.15	0.38	0.06
Mean		0.03	0.03	0.02	0.14	0.42	0.07
Std		0.00	0.00	0.00	0.01	0.04	0.01

Table B16. Injury Metric – Anterior Cruciate Ligament (ACL) Tension Force (N) (IARV = 1725 N†)

Loading Polarity		Away			Towards		
Loading Pulse		2.0g/50ms	2.7g/150ms	5.0g/10ms	2.0g/50ms	2.7g/150ms	5.0g/10ms
Loading Direction	Vertical	217.12	338.59	98.82	0.00	31.06	0.00
	Ant-Post 10°	216.69	336.77	98.14	0.00	4.08	0.00
	Ant-Post -10°	212.20	329.95	94.59	0.00	8.73	0.00
	Lateral 10°	218.33	346.30	96.57	0.00	0.00	0.00
	Lateral -10°	211.45	319.39	99.82	0.00	12.51	0.00
Mean		215.16	334.20	97.59	0.00	11.28	0.00
Std		2.78	9.05	1.83	0.00	10.75	0.00

† IARV represents ligament rupture/avulsion

Table B17. Injury Metric – Anterior Cruciate Ligament (ACL) Compression Force (N)

Loading Polarity		Away			Towards		
Loading Pulse		2.0g/50ms	2.7g/150ms	5.0g/10ms	2.0g/50ms	2.7g/150ms	5.0g/10ms
Loading Direction	Vertical	-0.02	-0.13	0.00	-100.55	-140.43	-71.26
	Ant-Post 10°	-0.02	-0.16	0.00	-100.86	-127.46	-73.69
	Ant-Post -10°	-0.02	-0.70	0.00	-96.52	-122.60	-61.61
	Lateral 10°	-0.02	-10.31	0.00	-97.58	-123.67	-77.57
	Lateral -10°	-0.02	-23.01	0.00	-98.60	-143.13	-65.14
Mean		-0.02	-6.86	0.00	-98.82	-131.46	-69.85
Std		0.00	8.95	0.00	1.67	8.62	5.77

Table B18. Injury Metric – Posterior Cruciate Ligament (PCL) Tension Force (N) (IARV = 1627 N†)

Loading Polarity		Away			Towards		
Loading Pulse		2.0g/50ms	2.7g/150ms	5.0g/10ms	2.0g/50ms	2.7g/150ms	5.0g/10ms
Loading Direction	Vertical	77.59	147.47	23.95	103.81	254.90	58.42
	Ant-Post 10°	76.45	125.20	21.75	106.95	209.98	59.96
	Ant-Post -10°	75.99	142.79	24.92	96.44	253.27	51.89
	Lateral 10°	62.45	128.32	20.98	101.02	192.83	57.95
	Lateral -10°	77.88	154.34	27.29	103.58	259.66	56.28
Mean		74.07	139.62	23.78	102.36	234.13	56.90
Std		5.85	11.17	2.26	3.51	27.35	2.77

† IARV represents ligament rupture/avulsion

Table B19. Injury Metric – Lateral Collateral Ligament (LCL) Tension Force (N) (IARV = 571 N†)

Loading Polarity		Away			Towards		
Loading Pulse		2.0g/50ms	2.7g/150ms	5.0g/10ms	2.0g/50ms	2.7g/150ms	5.0g/10ms
Loading Direction	Vertical	78.63	115.86	17.46	20.06	58.78	3.97
	Ant-Post 10°	76.47	113.06	15.98	20.68	54.32	4.45
	Ant-Post -10°	78.31	114.45	17.64	18.79	64.49	2.66
	Lateral 10°	76.55	113.09	21.44	23.82	72.01	4.64
	Lateral -10°	79.43	114.01	25.41	23.48	46.99	2.49
Mean		77.88	114.09	19.59	21.36	59.32	3.64
Std		1.17	1.03	3.43	1.96	8.55	0.90

† IARV represents ligament rupture/avulsion

Table B20. Injury Metric – Medial Collateral Ligament (MCL) Tension Force (N) (IARV = 1215 N†)

Loading Polarity		Away			Towards		
Loading Pulse		2.0g/50ms	2.7g/150ms	5.0g/10ms	2.0g/50ms	2.7g/150ms	5.0g/10ms
Loading Direction	Vertical	25.26	47.52	8.84	5.36	38.81	1.51
	Ant-Post 10°	24.39	41.58	8.49	8.14	24.13	2.21
	Ant-Post -10°	26.02	46.82	9.84	5.52	37.38	1.38
	Lateral 10°	28.73	48.38	10.88	7.66	34.34	2.50
	Lateral -10°	34.53	58.02	13.82	7.23	25.46	2.22

Mean	27.79	48.46	10.37	6.78	32.02	1.97
Std	3.67	5.33	1.91	1.14	6.09	0.44

[†] IARV represents ligament rupture/avulsion